Oxy-chromium-dravite, NaCr₃(Cr₄Mg₂)(Si₆O₁₈)(BO₃)₃(OH)₃O, a new mineral species of the tourmaline supergroup

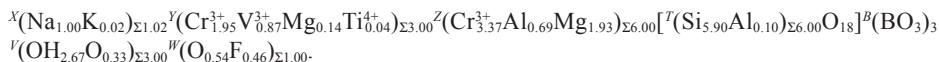**Ferdinando Bosi,[1,*] Leonid Reznitskii,[2] and Henrik Skogby[3]**

[1]Dipartimento di Scienze della Terra, Sapienza Università di Roma, P.le A. Moro, 5, I-00185 Rome, Italy
[2]Russian Academy of Science, Siberian Branch, Institute of the Earth's Crust, Lermontova Street, 128, Irkutsk, Russia
[3]Department of Mineralogy, Swedish Museum of Natural History, Box 50007, SE-10405 Stockholm, Sweden

Abstract

Oxy-chromium-dravite, NaCr₃(Cr₄Mg₂)(Si₆O₁₈)(BO₃)₃(OH)₃O, is a new mineral of the tourmaline supergroup. It is found in metaquartzites of the Pereval marble quarry (Sludyanka, Lake Baikal, Russia) in association with quartz, calcite, chromphyllite, eskolaite, chromite, uvarovite, chromian phlogopite, and pyroxenes of the diopside-kosmochlor series, Cr-bearing tremolite, Cr-bearing titanite, Cr-bearing rutile, and pyrite. Crystals are emerald green, transparent with a vitreous luster, green streak, and conchoidal fracture. Oxy-chromium-dravite has a VHN hardness of 14 540 MPa, a Mohs hardness of approximately 7½, and a calculated density of 3.3 g/cm³. In plane-polarized light, oxy-chromium-dravite is pleochroic (O = dark green, E = yellow green) and uniaxial negative: ω = 1.765(5), ε = 1.715(5). Oxy-chromium-dravite is rhombohedral, space group $R3m$, with the unit-cell parameters a = 16.1121(3), c = 7.3701(1) Å, V = 1656.95(5) Å³, Z = 3. The chemical characterization resulted in: SiO₂ = 31.73, TiO₂ = 0.31, B₂O₃ = 9.35, Al₂O₃ = 3.61, Cr₂O₃ = 36.25, V₂O₃ = 5.81, MgO = 7.49, Na₂O = 2.78, K₂O = 0.08, F = 0.78, H₂O = 2.16, sum 100.01 wt%. The unit formula is

$$^X(Na_{1.00}K_{0.02})_{\Sigma1.02}{}^Y(Cr^{3+}_{1.95}V^{3+}_{0.87}Mg_{0.14}Ti^{4+}_{0.04})_{\Sigma3.00}{}^Z(Cr^{3+}_{3.37}Al_{0.69}Mg_{1.93})_{\Sigma6.00}[^T(Si_{5.90}Al_{0.10})_{\Sigma6.00}O_{18}]^B(BO_3)_3$$
$$^V(OH_{2.67}O_{0.33})_{\Sigma3.00}{}^W(O_{0.54}F_{0.46})_{\Sigma1.00}.$$

The crystal structure of oxy-chromium-dravite was refined to statistical index R1 for all reflections equal to 1.54% using Mo$K\alpha$ X-ray intensity data. Oxy-chromium-dravite is related to chromium-dravite, ideally NaMg₃Cr₆(Si₆O₁₈)(BO₃)₃(OH)₃OH, by the heterovalent substitution $Cr^{3+}+O^{2-} \rightarrow Mg^{2+}+OH^{1-}$.

Keywords: Oxy-chromium-dravite, tourmaline, new mineral species, crystal-structure refinement, electron microprobe

Introduction

The tourmaline supergroup minerals are widespread, occurring in a wide variety of sedimentary, igneous, and metamorphic rocks. They are known as valuable indicator minerals that can provide information on the compositional evolution of their host rocks, chiefly due to their ability to incorporate a large number of elements (e.g., Novák et al. 2004, 2011; Agrosì et al. 2006; Lussier et al. 2011a; van Hinsberg et al. 2011). However, the chemical composition of tourmalines is also strongly controlled by various crystal-structural constraints (e.g., Hawthorne 1996, 2002; Bosi 2010, 2011) as well as by temperature (van Hinsberg and Schumacher 2011). Tourmaline supergroup minerals are complex borosilicates and their crystal structure and crystal chemistry have been widely studied (e.g., Foit 1989; Hawthorne and Henry 1999; Bosi and Lucchesi 2007; Lussier et al. 2008, 2011b; Bosi et al. 2010). The general formula of tourmaline may be formalized as: $XY_3Z_6T_6O_{18}(BO_3)_3V_3W$, where $^{[9]}X$ = Na, Ca, □ (= vacancy), K; $^{[6]}Y$ = Al, Fe³⁺, Cr³⁺, V³⁺, Mg, Fe²⁺, Mn²⁺, Li, Ti⁴⁺; $^{[6]}Z$ = Al, Fe³⁺, Cr³⁺, V³⁺, Mg, Fe²⁺; $^{[4]}T$ = Si, Al, B; $^{[3]}B$ = B; $^{[3]}V(\equiv O3)$ = OH, O; $^{[3]}W(\equiv O1)$ = OH, F, O. The dominance

of these ions at one or more sites of the structure gives rise to a range of distinct mineral species (Henry et al. 2011).

Although the compositions of most tourmalines correspond to the schorl-dravite-elbaite composition fields, cations that normally occur in low concentrations, such as chromium, may reach significant contents. Cr-bearing tourmalines were described in the 19th century (Cossa and Arzruni 1883) and are nowadays known from many regions throughout the world, occurring in various geological settings: e.g., mica schists (Dunn 1977); chromitites (Michailidis et al. 1995); ultramafic rocks (Grapes and Palmer 1996); metacarbonate rocks (Torres-Ruiz et al. 2003); and carbonate-altered ultramafic rocks (Peltonen et al. 2008; Arif et al. 2010). Chromium-dravite (described as chromdravite), ideally NaMg₃Cr₆(Si₆O₁₈)(BO₃)₃(OH)₃OH, was discovered in 1983 in Karelia, Russia (Rumyantseva 1983). The subsequent crystal-structural studies of this tourmaline suggested that Cr and Mg may be disordered over the Y and Z sites (Gorskaya et al. 1984; Rozhdestvenskaya et al. 2011). Recently, an Al-rich chromium-dravite was found in talc-tremolite-cummingtonite schist at the no. 1 mine at Balmat in the Adirondack Lowlands, St. Lawrence County, New York (Lupulescu and Rowe 2011). A new tourmaline species with Cr and Al dominant, respectively, at the Y and Z sites was found from the chromite deposits of

---

* E-mail: ferdinando.bosi@uniroma1.it

Nausahi, Keonjhar District, Orissa, India, and was given the name chromo-alumino-povondraite, ideally $NaCr_3(Al_4Mg_2)(Si_6O_{18})(BO_3)_3(OH)_3O$ (IMA 2009-088; Henry et al. 2011). Very Cr-rich tourmalines belonging to the oxy-subgroup 3 (Henry et al. 2011) were found in metamorphic rocks of the Sludyanka crystalline complex, on the southern shore of Lake Baikal (Reznitskii et al. 1988). The subsequent structural examination of these oxy-tourmalines demonstrated that Cr^{3+} can occur as the dominant cation at both the Y and Z sites, as shown for the sample TMt3b reported by Bosi et al. (2004). This sample was at first classified as chromium-dravite, but according to the current tourmaline nomenclature (Henry et al. 2011), its chemical composition is consistent with a new species, named oxy-chromium-dravite, with the ideal formula $NaCr_3(Cr_4Mg_2)(Si_6O_{18})(BO_3)_3(OH)_3O$.

The new species as well as the new name have been approved by the Commission on New Minerals, Nomenclature and Classification of the International Mineralogical Association (IMA 2011-097). The holotype specimen of oxy-chromium-dravite (sample TMt3b) is deposited in the collections of the Museum of Mineralogy, Earth Sciences Department, Sapienza University of Rome, Italy, catalog number 33064. A formal description of the new species oxy-chromium-dravite is presented here, including a full characterization of its physical, chemical, and structural attributes. However, after the sample TMt3b ($Cr_2O_3 = 30.9$ wt%) was approved as a new mineral species by the CNMNC-IMA, another sample showing the highest contents of Cr_2O_3 (36.3 wt%) so far reported for tourmaline in the literature was found from the same locality. Consequently, we will here present chemical and structural data of this new sample, T89102, which better represents the oxy-chromium-dravite end-member. Details on the chemical and structural data of sample TMt3b are reported in Bosi et al. (2004).

GEOLOGICAL SETTING

The Sludyanka crystalline complex is part of the Central Asian foldbelt, located in the Southern Lake Baikal region near the boundary between the foldbelt and the Siberian Craton. The Sludyanka complex comprise the Sludyanka and Khangarul Groups of sedimentary-metamorphic rocks consisting of diverse gneisses, carbonate, and carbonate-silicate rocks and mafic schists. The rocks underwent mainly granulite-facies regional metamorphism at ~800 °C and ~6–8 kbar, as well as a post-granulite metamorphic episode accompanied by weak to medium amphibolite-facies retrograde metamorphism. The regional metamorphism occurred in the Early Ordovician (Salnikova et al. 1998) upon a Riphean or, probably, Cambrian protolith (Kovach et al. 2011). Chromium-vanadium mineralizations occur in certain types of the Sludyanka metamorphites jointly referred to as quartz-diopside rocks. They make up 7–8% of the Sludyanka Group and are present throughout the section as layers of more or less complex structure with thicknesses from a few meters up to 100–200 m. All the rock varieties have simple chemical and mineralogical compositions and consist of pure white diopside, quartz, and calcite. Variations in mineral percentages produce a broad range of rock types, from calcite-diopside and quasi-monomineral diopsidite to quartzite and predominant foliated-banded quartz-diopside rocks, which gave the name to the group. The quartz-diopside group of rocks quite often

includes metaphosphorite with rock-forming apatite (from 1–2 to 50–60 wt%) and specific Cr-V-mineralization present in all quartz-diopside varieties and layers. The Cr and V concentrations produce an extremely broad range of Cr-V-bearing minerals, including silicates (clinopyroxene, amphibole, garnet, micas, chlorite, clinozoisite-epidote series, tourmaline), simple and complex Cr-V, Cr-V-Fe, Cr-V-Ti, Ba-Cr-V, and Mg-Fe-Cr-V oxides (eskolaite-karelianite, rutile, spinel, etc.), and sulfospinels (Reznitsky and Sklyarov 1996). The compositions are commonly inhomogeneous at all scales, within a hand specimen as well as within a fine grain. It is considered that Cr and V were available in the original sediments, the source of Cr and V (as well as phosphorus) being underwater volcanic exhalations.

Accessory tourmaline is found in every quartz-bearing variety of this rock series. Considering the equilibrium assemblages with the majority of the minerals, the tourmalines belong to the granulite stage of the metamorphism. They show considerable variation in Cr_2O_3, V_2O_3, and Al_2O_3 with Cr-rich tourmalines located in the rocks with high Cr/V and/or (Cr+V)/Al ratios, where they form joins between oxy-dravite and oxy-chromium-dravite or oxy-chromium-dravite and oxy-vanadium-dravite. The tourmalines occur mainly as zoned euhedral and subhedral prismatic crystals up to 100–300 μm in lengths (Figs. 1 and 2). Occasionally, homogeneous crystals can be found (2–3 grains out of 100).

OCCURRENCE, APPEARANCE, AND PHYSICAL AND OPTICAL PROPERTIES

The oxy-chromium-dravite occurs in the Pereval marble quarry, near the town of Sludyanka (51°37′N 103°38′E), Irkutsk region, Southern Lake Baikal, Siberia, Russia. The Pereval quarry is the type locality for natalyite, florensovite, kalininite, magnesiocoulsonite, vanadium-dravite, batisivite, oxyvanite, and cuprokalininite. Oxy-chromium-dravite was found in the two rock-types: chromphyllite-bearing quartzite (sample TMt3b) and banded quartz-diopside rock (T89102). Associated minerals in the quartzite are rock-forming quartz, calcite, chromphyllite, eskolaite, chromite, uvarovite, chromian phlogopite and pyroxenes of the diopside-kosmochlor series, Cr-bearing tremolite,
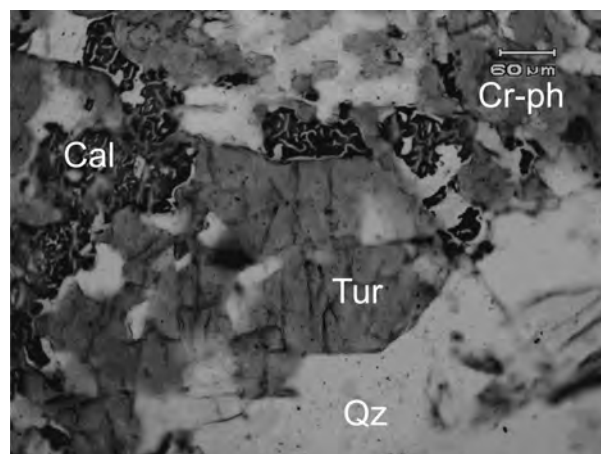

FIGURE 1. Microcrystal of the tourmaline in intergrowth with quartz, calcite, and chromphyllite from the quartzite (thin section).
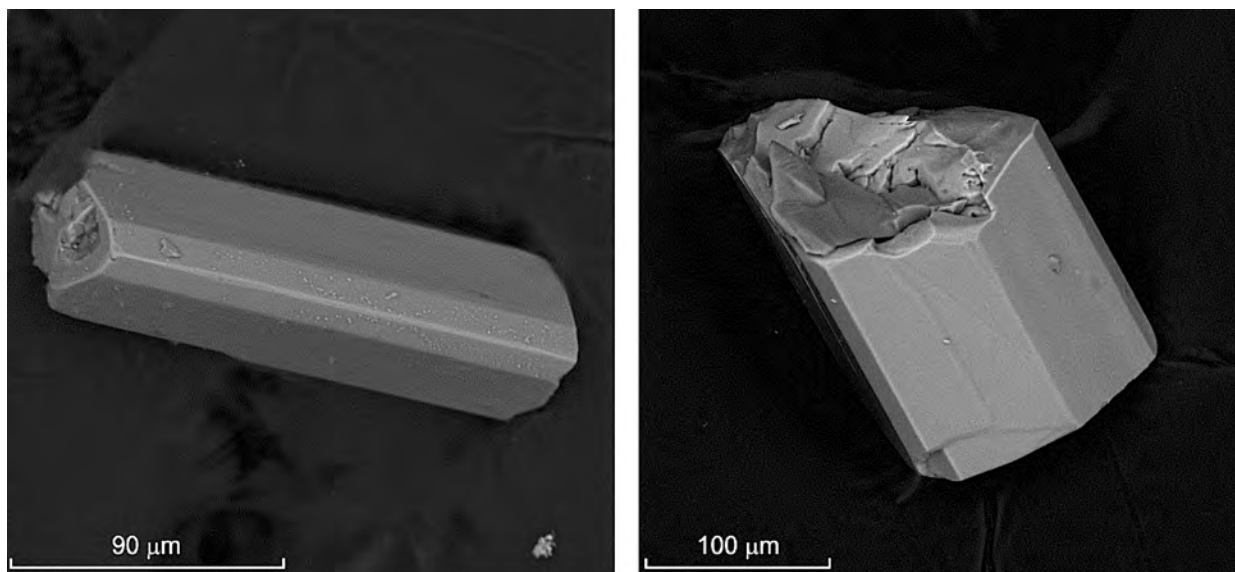
FIGURE 2. SEM images of the euhedral crystals of the Cr-rich tourmaline, collected from the quartzite.

Cr-bearing titanite, Cr-bearing rutile, and pyrite. The assemblage of the quartz-diopside rocks is more simple with Cr-V-bearing diopside, quartz, calcite, magnesiochromite, and escolaite-karelianite. One homogeneous crystal of oxy-chromium-dravite and many zoned ones in each rock type were found. The crystals of oxy-chromium-dravite are euhedral and inclusion-free, reaching up to 0.3 mm in size.

The oxy-chromium-dravite morphology consists of elongated $\{10\bar{1}0\}$ and $\{11\bar{2}0\}$ prisms terminated by a prominent $\{0001\}$ pedion and small, minor $\{10\bar{1}1\}$ pyramidal faces. Crystals are emerald green, with green streak, transparent, and display vitreous luster. They are brittle and show conchoidal fracture. The VHN microhardness is 14 540 MPa (load 50 g), equivalent to a Mohs hardness of approximately 7½ (Reznitsky et al. 2001). The calculated density is 3.299 and 3.315 g/cm³ for samples TMt3b and T89102, respectively. In transmitted light, oxy-chromium-dravite is pleochroic with O = dark green and E = yellow-green. Oxy-chromium-dravite is uniaxial negative with refractive indices, measured by the immersion method using white light from a tungsten source, of $\omega = 1.765(5)$ and $\varepsilon = 1.715(5)$ (sample TMt3b).

METHODS

Single-crystal structural refinement

A representative crystal of the type specimen material (sample T89102) was selected for X-ray diffraction measurements on a Bruker KAPPA APEX-II single-crystal diffractometer, at Sapienza University of Rome (Earth Sciences Department), equipped with a CCD area detector (6.2 × 6.2 cm² active detection area, 512 × 512 pixels) and a graphite crystal monochromator, using Mo$K\alpha$ radiation from a fine-focus sealed X-ray tube. The sample-to-detector distance was 4 cm. A total of 3265 exposures (step = 0.2°, time/step = 20 s) covering a full reciprocal sphere with a high redundancy of about 8 was used. Final unit-cell parameters were refined by means of the Bruker AXS SAINT program using reflections with $I > 10$ $\sigma(I)$ in the range 5°< 2θ <74°. The intensity data were processed and corrected for Lorentz, polarization, and background effects with the APEX2 software program of Bruker AXS. The data were corrected for absorption using the multiscan method (SADABS). The absorption correction led to a significant improvement in R_{int}. No violations of $R3m$ symmetry were noted.

Structural refinement was carried out with the SHELXL-97 program (Sheldrick 2008). Starting coordinates were taken from Bosi et al. (2004). Variable parameters were: scale factor, extinction coefficient, atomic coordinates, site-scattering values, and atomic displacement factors. To obtain the best values of statistical indexes ($R1$, $wR2$), a fully ionized scattering curve for O was used, whereas neutral scattering curves were used for the other atoms. In detail, the X and Y site were modeled by using Na and Cr scattering factors (respectively), while the occupancy of the Z site was modeled considering the presence of Cr and Mg. The T and B sites were modeled, respectively, with Si and B scattering factors and with a fixed occupancy of 1, because refinement with unconstrained occupancies showed no significant deviations from this value. Three full-matrix refinement cycles with isotropic displacement parameters for all atoms were followed by anisotropic cycles until convergence was attained. No significant correlations over a value of 0.7 between the parameters were observed at the end of refinement. Table 1 lists crystal data, data collection information, and refinement details; Table 2 gives the fractional

TABLE 1. Single-crystal X-ray diffraction data details for oxy-chromium-dravite

Sample T89102	
Crystal size (mm)	0.15 × 0.21 × 0.28
a (Å)	16.1121(3)
c (Å)	7.3701(1)
V (Å³)	1656.95(5)
Range for data collection, 2θ (°)	5–74
Reciprocal space range hkl	$-26 \le h \le 26$
	$-26 \le k \le 26$
	$-10 \le l \le 12$
Total number of frames	3265
Set of measured reflections	8088
Unique reflections, R_{int} (%)	1729, 2.38
Absorption correction method	Multiscan
Refinement method	Full-matrix last-squares on F^2
Structural refinement program	SHELXL-97
Extinction coefficient	0.00047(6)
Flack parameter	0.05(1)
w$R2$ (%)	2.79
$R1$ (%) all data	1.54
$R1$ (%) for $I > 2\sigma_I$	1.45
GooF	1.023
Diff. Peaks ($\pm e^-$/Å³)	0.35; −0.36

Notes: R_{int} = merging residual value; $R1$ = discrepancy index, calculated from F-data; $wR2$ = weighted discrepancy index, calculated from F^2-data; GooF = goodness of fit; Diff. Peaks = maximum and minimum residual electron density. Radiation, Mo$K\alpha$ = 0.71073 Å. Data collection temperature = 293 K. Space group $R3m$; $Z = 3$.

Table 2. Fractional atomic coordinates (x,y,z) and site occupancies for oxy-chromium-dravite

Site	x	y	z	Site occupancy
			Sample T89102	
X	0	0	0.2270(2)	$Na_{1.023(7)}$
Y	0.123083(17)	$x/2$	0.63874(5)	$Cr_{0.9649(18)}$
Z	0.297600(15)	0.261475(15)	0.60855(5)	$Cr_{0.564(2)}Mg_{0.436(2)}$
B	0.10930(6)	$2x$	0.4548(2)	$B_{1.00}$
T	0.189436(18)	0.187762(19)	0	$Si_{1.00}$
O1	0	0	0.7649(3)	$O_{1.00}$
O2	0.06015(4)	$2x$	0.49116(16)	$O_{1.00}$
O3	0.25501(8)	$x/2$	0.50900(16)	$O_{1.00}$
O4	0.09250(4)	$2x$	0.07148(16)	$O_{1.00}$
O5	0.18209(8)	$x/2$	0.09007(15)	$O_{1.00}$
O6	0.19072(5)	0.18146(5)	0.78133(11)	$O_{1.00}$
O7	0.28246(5)	0.28199(5)	0.07220(12)	$O_{1.00}$
O8	0.20649(5)	0.26678(6)	0.43700(12)	$O_{1.00}$
H3	0.2507(14)	0.1253(7)	0.376(3)	$H_{1.00}$

Notes: The column "site occupancy" denotes the elements whose scattering factors were used to determine the electron occupancy of the site.

Table 4. Selected bond distances (Å) in oxy-chromium-dravite

	Sample T89102		
B-O8^A ($\times$2)	1.3624(11)	Y-O1	1.9530(9)
B-O2	1.398(2)	Y-O6^C ($\times$ 2)	1.9798(8)
$<B$-O$>$	1.374	Y-O2^B ($\times$ 2)	2.0168(7)
		Y-O3	2.0744(11)
X-O2^{B,F} ($\times$3)	2.5707(15)	$<Y$-O$>$	2.003
X-O5^{B,F} ($\times$3)	2.7338(12)		
X-O4^{B,F} ($\times$3)	2.8244(13)	Z-O8^E	1.9660(8)
$<X$-O$>$	2.710	Z-O8	1.9714(8)
		Z-O7^E	1.9824(8)
T-O7	1.5997(7)	Z-O6	2.0073(8)
T*-O6	1.6156(8)	Z-O7^D	2.0079(8)
T-O4	1.6277(5)	Z-O3	2.0463(6)
T-O5	1.6427(5)	$<Z$-O$>$	1.997
$<T$-O$>$	1.621		
		O3-H3	0.98(2)

Notes: Standard uncertainty in parentheses. Superscript letters: A = ($y - x, y, z$); B = ($y - x, - x, z$); C = ($x, x - y, z$); D = ($y - x + 1/3, - x + 2/3, z + 2/3$); E = ($- y + 2/3, x - y + 1/3, z + 1/3$); F = ($- y, x - y, z$). Transformations relate coordinates to those of Table 2. * Positioned in adjacent unit cell.

Table 3. Displacement parameters (Å^2) for oxy-chromium-dravite

Site	U^{11}	U^{22}	U^{33}	U^{23}	U^{13}	U^{12}	U_{eq}
				Sample T89102			
X	0.0255(6)	0.0255(6)	0.0212(7)	0	0	0.0127(3)	0.0240(4)
Y	0.00427(11)	0.00430(8)	0.00604(10)	−0.00019(4)	−0.00037(7)	0.00213(5)	0.00487(6)
Z	0.00414(10)	0.00464(10)	0.00480(8)	0.00033(7)	−0.00014(6)	0.00215(8)	0.00455(6)
B	0.0054(5)	0.0056(6)	0.0080(6)	0.0008(5)	0.0004(2)	0.0028(3)	0.0063(3)
T	0.00451(13)	0.00431(12)	0.00567(12)	−0.00035(9)	−0.00024(10)	0.00208(9)	0.00489(6)
O1	0.0048(5)	0.0048(5)	0.0080(8)	0	0	0.0024(2)	0.0059(3)
O2	0.0044(3)	0.0041(4)	0.0074(5)	0.0013(3)	0.00066(17)	0.0021(2)	0.00532(19)
O3	0.0096(5)	0.0089(4)	0.0062(4)	0.00064(18)	0.0013(4)	0.0048(2)	0.00814(19)
O4	0.0068(3)	0.0150(5)	0.0083(4)	−0.0004(4)	−0.0002(2)	0.0075(3)	0.0091(2)
O5	0.0138(5)	0.0060(3)	0.0081(4)	0.00035(19)	0.0007(4)	0.0069(3)	0.00848(19)
O6	0.0075(3)	0.0060(3)	0.0046(3)	−0.0005(2)	−0.0001(2)	0.0030(3)	0.00620(13)
O7	0.0067(3)	0.0059(3)	0.0084(3)	−0.0015(3)	−0.0016(3)	0.0011(3)	0.00794(14)
O8	0.0051(3)	0.0085(3)	0.0132(3)	0.0035(3)	0.0007(3)	0.0034(3)	0.00893(15)
H3							0.012*

Notes: U^{ij} = anisotropic displacement parameter; U_{eq} = equivalent isotropic displacement parameters.
* Isotropic displacement parameter constrained to $1.5U_{eq}$(O3).

atomic coordinates and site occupancies; Table 3 gives the displacement parameters; Table 4 gives selected bond distances. (CIF[1] available on deposit.)

X-ray powder diffraction

A powder X-ray diffraction data pattern was derived from the single-crystal structural refinement since sufficient sample material for powder diffraction measurements was not available. The simulated X-ray powder diffraction data for oxy-chromium-dravite (samples T89102 and TMt3b) can be found in the American Mineralogist Crystal Structure Database (http://www.minsocam.org/MSA/Crystal_Database.html).

Electron microprobe analysis

Electron microprobe analyses of the crystal used for X-ray diffraction refinements were obtained by wavelength-dispersive spectroscopy with a Cameca SX50 instrument at the "Istituto di Geologia Ambientale e Geoingegneria (Rome, Italy), CNR", operating at an accelerating potential of 15 kV and a sample current of 15 nA. Minerals and synthetic compounds were used as standards: wollastonite (Si, Ca), magnetite (Fe), rutile (Ti), corundum (Al), fluorphlogopite (F), periclase (Mg), jadeite (Na), K-feldspar (K), sphalerite (Zn), metallic Cr, V, Mn, and Cu. V and Cr concentrations were corrected for interference from the Ti-$K\beta$ and V-$K\beta$ peaks, respectively. The PAP matrix correction procedure (Pouchou and Pichoir 1991) was applied to reduce the raw data. Each element determination was accepted after checking that the intensity obtained from the standards measured before and after each analytical session had not varied by more than 1%. The results, which are summarized in Table 5, represent mean values of 15 spot analyses. Figure 3 displays the compositional variations in Cr_2O_3, V_2O_3, and Al_2O_3 of the analyzed specimen. In accordance with the documented very low concentration of Li in dravitic samples (e.g., Henry et al. 2011), the Li_2O content was assumed to be insignificant. Fe, Mn, Zn, Cu, and Ca were found to be below their respective detection limits (0.03 wt%).

Results

Determination of atomic proportions

In agreement with the structural refinement results, the boron content was assumed to be stoichiometric in the sample of oxy-chromium-dravite (B = 3.00 apfu). In fact, both the site-scattering results and the bond lengths of B and T are consistent with the B site fully occupied by boron and no amount of B at the T site. The OH content can then be calculated by charge balance with the assumption $T + Y + Z = 15.00$. The atomic proportions were calculated on this assumption (Table 5). The excellent match between the number of electrons per formula unit (epfu) derived from chemical and structural analysis supports this procedure: 292.8 and 292.3 epfu, respectively

Site populations

The anion site populations in sample T89102 followed the general preference suggested for tourmaline (e.g., Grice and Ercit 1993; Henry et al. 2011): the O3 site (V position in the

TABLE 5. Chemical composition of oxy-chromium-dravite

Sample	T89102	TMt3b*
SiO₂ wt%	31.73(11)	32.54(33)
TiO₂	0.32(8)	0.03(1)
B₂O₃	9.35†	9.64†
Al₂O₃	3.61(41)	9.71(31)
Cr₂O₃	36.25(72)	30.92(45)
V₂O₃	5.81(58)	2.50(21)
FeO	–	0.32(6)
MgO	7.49(16)	8.33(8)
ZnO	–	0.13(7)
CaO	–	0.38(3)
Na₂O	2.78(7)	2.52(5)
K₂O	0.08(2)	0.07(1)
F	0.78(7)	0.67(5)
H₂O	2.16†	2.50†
–O=F	–0.33	–0.28
Total	100.01	99.98

Atomic proportions normalized to 31 anions		
Si apfu	5.90(9)	5.86(6)
Ti⁴⁺	0.04(1)	0.01(2)
B	3.00	3.00
Al	0.79(9)	2.06(5)
Cr³⁺	5.33(11)	4.41(6)
V³⁺	0.87(13)	0.36(3)
Fe²⁺	–	0.05(1)
Mg	2.07(5)	2.24(3)
Zn	–	0.02(1)
Ca	–	0.07(1)
Na	1.00(3)	0.88(3)
K	0.02(1)	0.02(0)
F	0.46(4)	0.38(3)
OH	2.67	3.01

Notes: Errors for oxides are standard deviations (in brackets) of 15 spot analyses. Standard errors for ions were calculated by error-propagation theory.
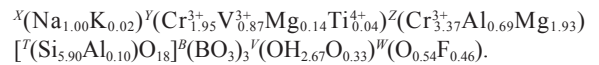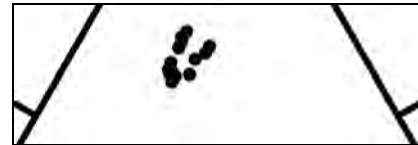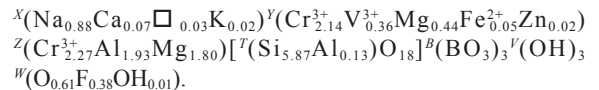* Data from Bosi et al. (2004).
† Calculated by stoichiometry.
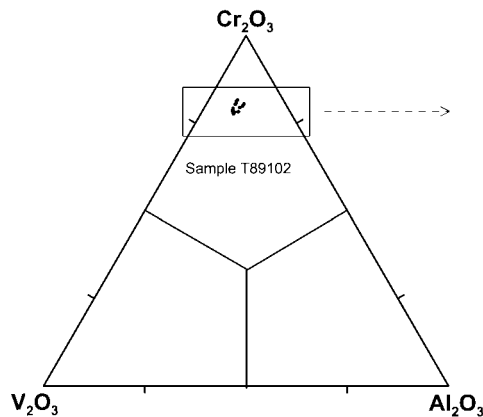
general formula) is occupied by OH and O^{2-}, while the O1 site (W position in the general formula) is occupied by O^{2-} and F. The cation distribution at the T, Y, and Z sites was optimized by using a quadratic program to minimize the residuals between calculated and observed data (based on the chemical and structural analysis). Site-scattering values, octahedral, and tetrahedral mean bond distances (i.e., <Y-O>, <Z-O>, and <T-O>) were calculated as the linear contribution of each cation multiplied by its specific bond distance (Table 6). More details about the specific distances as well as about the optimization procedure may be found in Bosi et al. (2004). The robustness of this approach was confirmed by another optimization procedure (Wright et al. 2000), which led to very similar cation distributions (Table 6). This result represents another example of convergence of these two procedures to similar solutions for tourmaline (e.g., Bosi, and Lucchesi 2007; Filip et al. 2012).

The final structural formula of sample T89102 is as follows:

$$^X(Na_{1.00}K_{0.02})^Y(Cr^{3+}_{1.95}V^{3+}_{0.87}Mg_{0.14}Ti^{4+}_{0.04})^Z(Cr^{3+}_{3.37}Al_{0.69}Mg_{1.93})$$
$$[^T(Si_{5.90}Al_{0.10})O_{18}]^B(BO_3)_3{}^V(OH_{2.67}O_{0.33})^W(O_{0.54}F_{0.46}).$$

For comparison, the structural formula of sample TMt3b (Bosi et al. 2004) with appropriate grouping of constituents is also reported:

$$^X(Na_{0.88}Ca_{0.07}\square_{0.03}K_{0.02})^Y(Cr^{3+}_{2.14}V^{3+}_{0.36}Mg_{0.44}Fe^{2+}_{0.05}Zn_{0.02})$$
$$^Z(Cr^{3+}_{2.27}Al_{1.93}Mg_{1.80})[^T(Si_{5.87}Al_{0.13})O_{18}]^B(BO_3)_3{}^V(OH)_3$$
$$^W(O_{0.61}F_{0.38}OH_{0.01}).$$

FIGURE 3. Ternary diagram for the Al_2O_3-V_2O_3-Cr_2O_3 system relative to the 15 spot EMP analyses of sample T89102.

TABLE 6. Cation site populations (apfu), site scattering factors (epfu), and mean bond distances (Å) for oxy-chromium-dravite

Site	Site population	Site scattering		Mean bond length	
		Observed	Calculated	Observed	Calculated
X	1.00 Na + 0.02 K	11.25(8)	11.38		
Y	1.95 Cr³⁺ + 0.87 V³⁺ + 0.14 Mg + 0.04 Ti⁴⁺	69.5(1)	69.4	2.003	1.995
	ᵞ(1.99 Cr³⁺ + 0.86 V³⁺ + 0.14 Mg + 0.02 Ti⁴⁺)*				
Z	3.37 Cr³⁺ + 0.69 Al + 1.93 Mg	112.6(3)	113.1	1.997	1.997
	ᶻ(3.33 Cr³⁺ + 0.73 Al + 1.94 Mg)*				
T	5.90 Si + 0.10 Al	84†	83.9	1.621	1.621
	ᵀ(5.92 Si + 0.08 Al)*				
B	3 B	15†	15		

Notes: O2, O4…O8 sites are fully populated by O^{2-}; apfu = atoms per formula unit; epfu = electrons per formula unit.
* Site populations optimized by the procedure of Wright et al. (2000) with the weights on bond length parameters set to zero.
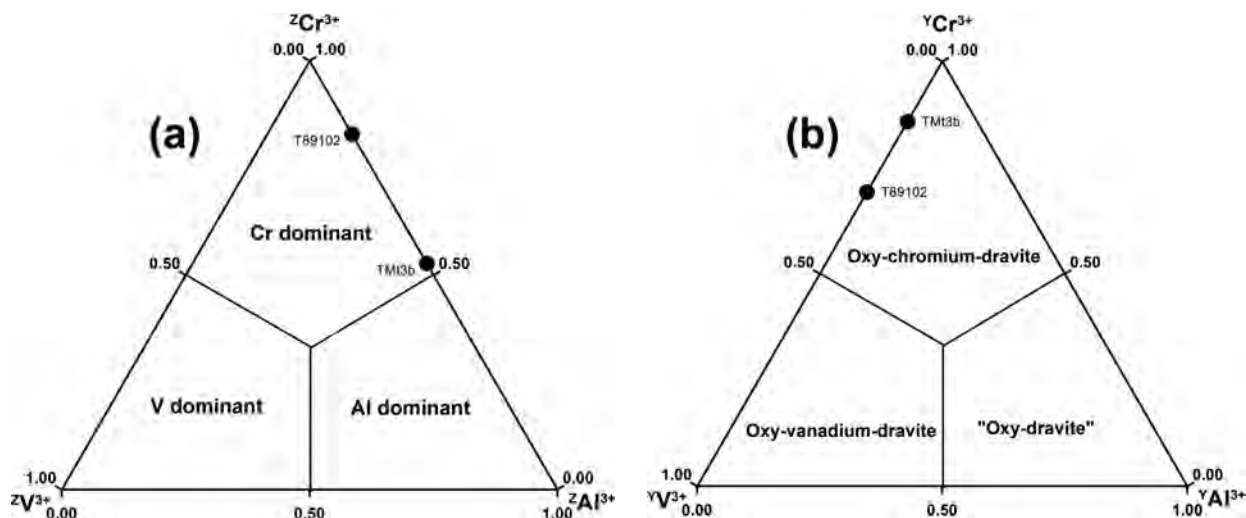† Fixed in the final stages of refinement.

FIGURE 4. Ternary diagram for the Al-V-Cr subsystem used for illustrating the dominant occupancy of the Z site (**a**) and Y site (**b**) for oxy-tourmaline.

DISCUSSION

The chemical composition of samples T89102 and TMt3b are consistent with tourmalines belonging to the alkali group, oxy-subgroup 3 (Henry et al. 2011). They are Na-dominant at the X position of the general formula, oxygen-dominant at W with $O^{2-} >$ OH+F, Cr^{3+} is the dominant trivalent cation at Y and Z, and Mg is the dominant divalent cation at Z. The ideal end-member may therefore be represented as $NaCr_3(Cr_4Mg_2)$ $Si_6O_{18}(BO_3)_3(OH)_3O$. Because no tourmalines have yet been documented as Cr^{3+}-dominant at Y and Z, this tourmaline can be classified as a new species (Fig. 4). By analogy with the relation between oxy-dravite (IMA 2012-004a) and dravite, as well as oxy-schorl and schorl, the name oxy-chromium-dravite is given in relation to chromium-dravite. In line with the above mentioned oxy-transitions, the prefix "oxy" represents the heterovalent substitution $Cr^{3+}+O^{2-} \rightarrow Mg^{2+} + OH^{1-}$ relative to the root composition of chromium-dravite. Comparative data for oxy-chromium-dravite and chromium-dravite are given in Table 7. Oxy-chromium-dravite is related to oxy-dravite by the homovalent substitution $Cr^{3+} \rightarrow$ Al at the Y and Z positions, and to chromo-alumino-povondraite by the substitution $Cr^{3+} \rightarrow$ Al at the Z position.

Concerning sample T89102, the X site is populated by the highest amount of Na (Table 5) so far reported for a tourmaline.

Given the low amounts of ^XK in sample T89102, the contribution of K to mean bond distance $<X$-$O> = 2.710$ should be insignificant. Consequently, an ideal distance for $<^XNa$-$O>$ approximately equal to 2.70 Å can be considered as representative of the X site fully occupied by Na. In contrast to Cr^{3+}, which is disordered over the Y and Z sites, Al (0.69 apfu) is essentially ordered at the Z site, although small amounts (=0.10 apfu) occupies the T site as well. V^{3+} (0.87 apfu) is completely ordered at the Y site, while Mg shows a clear preference for the Z site. From a crystallographic viewpoint, it is interesting to note that the mean bond distances $<Y$-$O>$ and $<Z$-$O>$ are rather similar in sample T89102 (2.003 and 1.997 Å, respectively). Their small difference ($\Delta_{Y-Z} = <Y$-$O> - <Z$-$O> = 0.006$ Å) is in excellent agreement with the positive correlation between the O3-Z-O6 angle and Δ_{Y-Z} observed by Bosi (2008): O3-Z-O6 $= 41.4141 \times \Delta_{Y-Z} + 78.5810$ ($r^2 = 0.92$). This relation yields a value of O3-Z-O6 $= 78.85°$ in line with the observed one of 79.77°. As reported by Bosi (2008) this correlation may be considered as a long-range structural constraint for tourmaline. If the O3-Z-O6 angle becomes larger, the shielding effect of the anions may be weakened and the repulsive force between the cations at Y and Z becomes greater. This may lead to instabilities in the tourmaline structure. However, incorporation of trivalent cations into the Y site and divalent cations into the Z site causes reduction of Δ_{Y-Z} as well as the O3-Z-O6 angle. In this way, the shielding effect needed to reduce the Y-Z repulsion may be provided, leading to energetic stabilization of structure.

REFERENCES CITED

Agrosì, G., Bosi, F., Lucchesi, S., Melchiorre, G., and Scandale, E. (2006) Mn-tourmaline crystals from island of Elba (Italy): Growth history and growth marks. American Mineralogist, 91, 944–952.

Arif, M., Henry, D.J., and Moon, C.J. (2010) Cr-bearing tourmaline associated with emerald deposits from Swat, NW Pakistan: Genesis and its exploration

TABLE 7. Comparative data for oxy-chromium-dravite and chromium-dravite

	Oxy-chromium-dravite	Chromium-dravite
a (Å)	16.0539(7)–16.1121(3)	16.11(1)
c	7.3247(5)–7.3701(1)	7.27(1)
V (Å^3)	1634.86(15)–1656.95(5)	1634.02
Space group	$R3m$	$R3m$
Optic sign	Uniaxial (–)	Uniaxial (–)
ω	1.765(5)	1.778(5)
ε	1.715(5)	1.772(5)
Streak	Green	Grayish green
Color	Emerald green	Dark emerald green to greenish black
Pleochroism	O = dark green	E = yellow green
	O = dark green	E = yellow green
Reference	Bosi et al. (2004); This work	Rumyantseva (1983)

significance. American Mineralogist, 95, 799–809.

Bosi, F. (2008) Disordering of Fe^{2+} over octahedrally coordinated sites of tourmaline. American Mineralogist, 93, 1647–1653.

——— (2010) Octahedrally coordinated vacancies in tourmaline: a theoretical approach. Mineralogical Magazine, 74, 1037–1044.

——— (2011) Stereochemical constraints in tourmaline: from a short-range to a long-range structure. Canadian Mineralogist, 49, 17–27.

Bosi, F. and Lucchesi, S. (2007) Crystal chemical relationships in the tourmaline group: structural constraints on chemical variability. American Mineralogist, 92, 1054–1063.

Bosi, F., Lucchesi, S., and Reznitskii, L. (2004) Crystal chemistry of the dravite-chromdravite series. European Journal of Mineralogy, 16, 345–352.

Bosi, F., Balić-Žunić, T., and Surour, A.A. (2010) Crystal structure analysis of four tourmalines from the Cleopatra's Mines (Egypt) and Jabal Zalm (Saudi Arabia), and the role of Al in the tourmaline group. American Mineralogist, 95, 510–518.

Cossa, A. and Arzruni, A. (1883) Chromturmalin aus den Chromeisenlagern des Ural. Zeitschrift für Krystallographie und Mineralogie, 7, 1–16.

Dunn, P.J. (1977) Chromium in dravite. Mineralogical Magazine, 41, 408–410.

Filip, J., Bosi, F., Novák, M., Skogby, H., Tuček, J., Čuda, J., and Wildner, M. (2012) Redox processes of iron in the tourmaline structure: example of the high-temperature treatment of Fe^{3+}-rich schorl. Geochimica et Cosmochimica Acta, 86, 239–256.

Foit, F.F. Jr. (1989) Crystal chemistry of alkali-deficient schorl and tourmaline structural relationships. American Mineralogist, 74, 422–431.

Gorskaya, M.G., Frank-Kamenetskaya, O.V., Rozhdestvenskaya, I.V., and Frank-Kamenetskii, V.A. (1984) Crystal structure of chromdravite, a new mineral. Proceedings 27th International Geological Congress, Moscow, Russia, 48–49.

Grapes, R. and Palmer, K. (1996) (Ruby-sapphire)-chromian mica-tourmaline rocks from Westland, New Zealand. Journal of Petrology, 37, 293–315.

Grice, J.D. and Ercit, T.S. (1993) Ordering of Fe and Mg in the tourmaline crystal structure: the correct formula. Neues Jahrbuch für Mineralogie Abhandlungen, 165, 245–266.

Hawthorne, F.C. (1996) Structural mechanisms for light-element variations in tourmaline. Canadian Mineralogist, 34, 123–132.

——— (2002) Bond-valence constraints on the chemical composition of tourmaline. Canadian Mineralogist, 40, 789–797.

Hawthorne, F.C. and Henry, D. (1999) Classification of the minerals of the tourmaline group. European Journal of Mineralogy, 11, 201–215.

Henry, D.J., Novák, M., Hawthorne, F.C., Ertl, A., Dutrow, B., Uher, P., and Pezzotta, F. (2011) Nomenclature of the tourmaline supergroup minerals. American Mineralogist, 96, 895–913.

Kovach, V.P., Salnikova, E.B., Wang, K.L., Jahn, B.M., Chiu, H.Y., Reznitskiy, L.Z., Kotov, A.B., Iizuka, Y., and Chung, S.L. (2011) Zircon ages and Hf isotopic constraints on sources of clastic metasediments of the Slyudyansky high-grade complex, southeastern Siberia: Implication for continental growth and evolution of the Central Asian Orogenic Belt. Journal of Asian Earth Sciences. http://dx.doi.org/10.1016/j.jseaes.2011.08.008.

Lupulescu, M. and Rowe, R. (2011) Chromo-alumino-povondraite from the 1 mine, Balmat, St. Lawrence County, New York. Canadian Mineralogist, 49, 1189–1198.

Lussier, A.J., Aguiar, P.M., Michaelis, V.K., Kroeker, S., Herwig, S., Abdu, Y., and Hawthorne, F.C. (2008) Mushroom elbaite from the Kat Chay mine, Momeik, near Mogok, Myanmar: I. Crystal chemistry by SREF, EMPA, MAS NMR and Mössbauer spectroscopy. Mineralogical Magazine, 72, 747–761.

Lussier, A.J., Hawthorne, F.C., Aguiar, P.M., Michaelis, V.K., and Kroeker, S. (2011a) Elbaite-liddicoatite from Black Rapids glacier, Alaska. Periodico di Mineralogia, 80, 57–73.

Lussier, A.J., Abdu, Y., Hawthorne, F.C., Michaelis, V.K., Aguiar, P.M., and Kroeker, S. (2011b) Oscillatory zoned liddicoatite from Anjanabonoina, central Madagascar. I. Crystal chemistry and structure by SREF and ^{11}B and ^{27}Al MAS NMR spectroscopy. Canadian Mineralogist, 49, 63–88.

Michailidis, K., Sklavounos, S., and Plimer, I. (1995) Chromian dravite from the chromite ores of Vavdos area, Chalkidiki peninsula, northern Greece. Neues Jahrbuch für Mineralogie Monatshefte, 513–528.

Novák, M., Povondra, P., and Selway, J.B. (2004) Schorl-oxy-schorl to dravite-oxy-dravite tourmaline from granitic pegmatites; examples from the Moldanubicum, Czech Republic. European Journal of Mineralogy, 16, 323–333.

Novák, M., Škoda, P., Filip, J., Macek, I., and Vaculovič, T. (2011) Compositional trends in tourmaline from intragranitic NYF pegmatites of the Tøebíč Pluton, Czech Republic; electron microprobe, Mössbauer, and LA-ICP-MS study. Canadian Mineralogist, 49, 359–380.

Peltonen, P., Kontinen, A., Huhma, H., and Kuronen, U. (2008) Outukumpu revisited: new mineral deposit model for the mantle peridotite-associated Cu–Co–Zn–Ni–Ag–Au sulphide deposits. Ore Geology Reviews, 33, 559–617.

Pouchou, J.L. and Pichoir, F. (1991) Quantitative analysis of homogeneous or stratified microvolumes applying the model "PAP." In K.F.J. Heinrich and D.E. Newbury, Eds., Electron Probe Quantitation, p. 31–75. Plenum, New York.

Reznitskii, L.Z., Sklyarov, E.V., and Ushapovskaya, Z.F. (1988) Minerals of chromium and vanadium in Sludyanka Crystalline Complex (southern Pribaikalia). In V.G. Belichenko, Ed., Metamorphic Formations of Pre-Cambrian of Eastern Siberia, p. 64–74. Nauka, Novosibirsk, Russia.

Reznitsky, L.Z. and Sklyarov, E.V. (1996) Unique Cr-V mineral association in metacarbonate rocks of the Sludyanka, Russia. 30th International Geological Congress, Beijing, China. Abstract, 2–3, 446.

Reznitsky, L.Z., Sklyarov, E.V., Ushchapovskaya, Z.V., Nartova, N.V., Kashaev, A.A., Karmanov, N.S., Kanakin, S.V., Smolin, A.S., and Nekrosova, E.A. (2001) Vanadiumdravite, $NaMg_3V_6[Si_6O_{18}][BO_3]_3(OH)_4$, a new mineral of the tourmaline group. Zapiski Vsesoyuznogo Mineralogicheskogo Obshchestva, 130, 59–72 (in Russian).

Rozhdestvenskaya, I.V., Vereshchagin, O.S., Frank-Kamenetskaya, O.V., Zolotarev, A.A., and Pekov, I.V. (2011) About crystal-chemical formula of chromdravite—mineral species from the tourmaline group. Zapiski Rossiiskogo Mineralogicheskogo Obshchestva (Proceedings of the Russian Mineralogical Society), 140, 93–99 (in Russian).

Rumyantseva, F.V. (1983) Chromdravite, a new mineral. Zapiski Vsesoyuznogo Mineralogicheskogo Obshchestva, 112, 222–226 (English summary in American Mineralogist, 69, 210).

Salnikova, E.B., Sergeev, S.A., Kotov, A.B., Yakovleva, S.Z., Steiger, R.H., Reznitskiy, L.Z., and Vasil'ev, E.P. (1998) U-Pb zircon dating of granulite metamorphism in the Slyudyanskiy complex, Eastern Siberia. Gondwana Research, 1, 195–205.

Sheldrick, G.M. (2008) A short history of SHELX. Acta Crystallographica A, 64, 112–122.

Torres-Ruiz, J., Pesquera, A., and López Sánchez-Vizcaíno, V. (2003) Chromian tourmaline and associated Cr-bearing minerals from the Nevado-Filábride Complex (Betic Cordilleras, SE Spain). Mineralogical Magazine, 67, 517–533.

van Hinsberg, V.J. and Schumacher, J.C. (2011) Tourmaline as a petrogenetic indicator mineral in the Haut-Allier metamorphic suite, Massif Central, France. Canadian Mineralogist, 49, 177–194.

van Hinsberg, V.J., Henry, D.J., and Marschall, H.R. (2011) Tourmaline: an ideal indicator of its host environment. Canadian Mineralogist, 49, 1–16.

Wright, S.E., Foley, J.A., and, Hughes, J.M. (2000) Optimization of site occupancies in minerals using quadratic programming. American Mineralogist, 85, 524–531.

```
data_T89102

_audit_creation_method                SHELXL-97
_chemical_name_systematic
;
 ?
;
_chemical_name_common                 ?
_chemical_melting_point               ?
_chemical_formula_moiety              ?
_chemical_formula_sum
 'H2.65 Al0.79 B3 Cr5.33 F0.46 K0.02 Mg2.08 Na O229.65 Si5.90 Ti0.04 V0.87'
_chemical_formula_weight              1102.69

loop_
 _atom_type_symbol
 _atom_type_description
 _atom_type_scat_dispersion_real
 _atom_type_scat_dispersion_imag
 _atom_type_scat_source
 'B'  'B'   0.0013   0.0007
 'International Tables Vol C Tables 4.2.6.8 and 6.1.1.4'
 'O'  'O2'  0.0080   0.0060
 'International Tables Vol C Tables 4.2.6.8 and 6.1.1.4'
 'Na' 'Na'  0.0362   0.0249
 'International Tables Vol C Tables 4.2.6.8 and 6.1.1.4'
 'Si' 'Si'  0.0817   0.0704
 'International Tables Vol C Tables 4.2.6.8 and 6.1.1.4'
 'Cr' 'Cr'  0.3209   0.6236
 'International Tables Vol C Tables 4.2.6.8 and 6.1.1.4'
 'Mg' 'Mg'  0.0486   0.0363
 'International Tables Vol C Tables 4.2.6.8 and 6.1.1.4'
 'H'  'H'   0.0000   0.0000
 'International Tables Vol C Tables 4.2.6.8 and 6.1.1.4'
 'F'  'F'   0.0171   0.0103
 'International Tables Vol C Tables 4.2.6.8 and 6.1.1.4'
 'K'  'K'   0.2009   0.2494
 'International Tables Vol C Tables 4.2.6.8 and 6.1.1.4'
 'V'  'V'   0.3005   0.5294
 'International Tables Vol C Tables 4.2.6.8 and 6.1.1.4'
 'Al' 'Al'  0.0645   0.0514
 'International Tables Vol C Tables 4.2.6.8 and 6.1.1.4'
 'Ti' 'Ti'  0.2776   0.4457
 'International Tables Vol C Tables 4.2.6.8 and 6.1.1.4'

_symmetry_cell_setting                ?
_symmetry_space_group_name_H-M        ?

loop_
 _symmetry_equiv_pos_as_xyz
 'x, y, z'
 '-y, x-y, z'
 '-x+y, -x, z'
 '-y, -x, z'
```

```
 '-x+y, y, z'
 'x, x-y, z'
 'x+2/3, y+1/3, z+1/3'
 '-y+2/3, x-y+1/3, z+1/3'
 '-x+y+2/3, -x+1/3, z+1/3'
 '-y+2/3, -x+1/3, z+1/3'
 '-x+y+2/3, y+1/3, z+1/3'
 'x+2/3, x-y+1/3, z+1/3'
 'x+1/3, y+2/3, z+2/3'
 '-y+1/3, x-y+2/3, z+2/3'
 '-x+y+1/3, -x+2/3, z+2/3'
 '-y+1/3, -x+2/3, z+2/3'
 '-x+y+1/3, y+2/3, z+2/3'
 'x+1/3, x-y+2/3, z+2/3'

_cell_length_a                    16.1121(3)
_cell_length_b                    16.1121(3)
_cell_length_c                    7.37010(10)
_cell_angle_alpha                 90.00
_cell_angle_beta                  90.00
_cell_angle_gamma                 120.00
_cell_volume                      1656.95(5)
_cell_formula_units_Z             3
_cell_measurement_temperature     293(2)
_cell_measurement_reflns_used     ?
_cell_measurement_theta_min       ?
_cell_measurement_theta_max       ?

_exptl_crystal_description        ?
_exptl_crystal_colour             ?
_exptl_crystal_size_max           0.30
_exptl_crystal_size_mid           0.21
_exptl_crystal_size_min           0.15
_exptl_crystal_density_meas       ?
_exptl_crystal_density_diffrn     3.315
_exptl_crystal_density_method     'not measured'
_exptl_crystal_F_000              1788
_exptl_absorpt_coefficient_mu     3.790
_exptl_absorpt_correction_type    ?
_exptl_absorpt_correction_T_min   0.3960
_exptl_absorpt_correction_T_max   0.6002
_exptl_absorpt_process_details    ?

_exptl_special_details
;
 ?
;

_diffrn_ambient_temperature       293(2)
_diffrn_radiation_wavelength      0.71073
_diffrn_radiation_type            MoK\a
_diffrn_radiation_source          'fine-focus sealed tube'
_diffrn_radiation_monochromator   graphite
_diffrn_measurement_device_type   ?
_diffrn_measurement_method        ?
```

```
_diffrn_detector_area_resol_mean    ?
_diffrn_standards_number            ?
_diffrn_standards_interval_count    ?
_diffrn_standards_interval_time     ?
_diffrn_standards_decay_%           ?
_diffrn_reflns_number               8088
_diffrn_reflns_av_R_equivalents     0.0238
_diffrn_reflns_av_sigmaI/netI       0.0270
_diffrn_reflns_limit_h_min          -26
_diffrn_reflns_limit_h_max          26
_diffrn_reflns_limit_k_min          -26
_diffrn_reflns_limit_k_max          26
_diffrn_reflns_limit_l_min          -10
_diffrn_reflns_limit_l_max          12
_diffrn_reflns_theta_min            2.53
_diffrn_reflns_theta_max            37.05
_reflns_number_total                1729
_reflns_number_gt                   1681
_reflns_threshold_expression        >2sigma(I)

_computing_data_collection          ?
_computing_cell_refinement          ?
_computing_data_reduction           ?
_computing_structure_solution       'SHELXS-97 (Sheldrick, 1990)'
_computing_structure_refinement     'SHELXL-97 (Sheldrick, 1997)'
_computing_molecular_graphics       ?
_computing_publication_material     ?

_refine_special_details
;
 Refinement of F^2^ against ALL reflections.  The weighted R-factor wR and
 goodness of fit S are based on F^2^, conventional R-factors R are based
 on F, with F set to zero for negative F^2^. The threshold expression of
 F^2^ > 2sigma(F^2^) is used only for calculating R-factors(gt) etc. and is
 not relevant to the choice of reflections for refinement.  R-factors based
 on F^2^ are statistically about twice as large as those based on F, and R-
 factors based on ALL data will be even larger.
;

_refine_ls_structure_factor_coef    Fsqd
_refine_ls_matrix_type              full
_refine_ls_weighting_scheme         calc
_refine_ls_weighting_details
 'calc w=1/[\s^2^(Fo^2^)+(0.0088P)^2^+0.0000P] where P=(Fo^2^+2Fc^2^)/3'
_atom_sites_solution_primary        direct
_atom_sites_solution_secondary      difmap
_atom_sites_solution_hydrogens      geom
_refine_ls_hydrogen_treatment       mixed
_refine_ls_extinction_method        SHELXL
_refine_ls_extinction_coef          0.00047(6)
_refine_ls_extinction_expression
 'Fc^*^=kFc[1+0.001xFc^2^\l^3^/sin(2\q)]^-1/4^'
_refine_ls_abs_structure_details
 'Flack H D (1983), Acta Cryst. A39, 876-881'
_refine_ls_abs_structure_Flack      0.054(11)
```

```
_refine_ls_number_reflns           1729
_refine_ls_number_parameters       94
_refine_ls_number_restraints       0
_refine_ls_R_factor_all            0.0154
_refine_ls_R_factor_gt             0.0145
_refine_ls_wR_factor_ref           0.0279
_refine_ls_wR_factor_gt            0.0277
_refine_ls_goodness_of_fit_ref     1.023
_refine_ls_restrained_S_all        1.023
_refine_ls_shift/su_max            0.001
_refine_ls_shift/su_mean           0.000

loop_
 _atom_site_label
 _atom_site_type_symbol
 _atom_site_fract_x
 _atom_site_fract_y
 _atom_site_fract_z
 _atom_site_U_iso_or_equiv
 _atom_site_adp_type
 _atom_site_occupancy
 _atom_site_symmetry_multiplicity
 _atom_site_calc_flag
 _atom_site_refinement_flags
 _atom_site_disorder_assembly
 _atom_site_disorder_group
NaX Na 0.0000 0.0000 0.2270(2) 0.0240(4) Uani 1.023(7) 6 d SP . .
CrY Cr 0.123083(17) 0.061541(8) 0.63874(5) 0.00487(6) Uani 0.9649(18) 2 d SP . .
MgZ Mg 0.297600(15) 0.261475(15) 0.60855(5) 0.00455(6) Uani 0.436(2) 1 d P . .
CrZ Cr 0.297600(15) 0.261475(15) 0.60855(5) 0.00455(6) Uani 0.564(2) 1 d P . .
B B 0.10930(6) 0.21861(12) 0.4548(2) 0.0063(3) Uani 1 2 d S . .
Si Si 0.189436(18) 0.187762(19) 0.0000 0.00489(6) Uani 1 1 d . . .
O1 O2 0.0000 0.0000 0.7649(3) 0.0059(3) Uani 1 6 d S . .
O2 O2 0.06015(4) 0.12030(7) 0.49116(16) 0.00532(19) Uani 1 2 d S . .
O3 O2 0.25501(8) 0.12751(4) 0.50900(16) 0.00814(19) Uani 1 2 d S . .
H3 H 0.2507(14) 0.1253(7) 0.376(3) 0.012 Uiso 1 2 d S . .
O4 O2 0.09250(4) 0.18500(8) 0.07148(16) 0.0091(2) Uani 1 2 d S . .
O5 O2 0.18209(8) 0.09105(4) 0.09007(15) 0.00848(19) Uani 1 2 d S . .
O6 O2 0.19072(5) 0.18146(5) 0.78133(11) 0.00620(13) Uani 1 1 d . . .
O7 O2 0.28246(5) 0.28199(5) 0.07220(12) 0.00794(14) Uani 1 1 d . . .
O8 O2 0.20649(5) 0.26678(6) 0.43700(12) 0.00893(15) Uani 1 1 d . . .

loop_
 _atom_site_aniso_label
 _atom_site_aniso_U_11
 _atom_site_aniso_U_22
 _atom_site_aniso_U_33
 _atom_site_aniso_U_23
 _atom_site_aniso_U_13
 _atom_site_aniso_U_12
NaX 0.0255(6) 0.0255(6) 0.0212(7) 0.000 0.000 0.0127(3)
CrY 0.00427(11) 0.00430(8) 0.00604(10) -0.00019(4) -0.00037(7) 0.00213(5)
MgZ 0.00414(10) 0.00464(10) 0.00480(8) 0.00033(7) -0.00014(6) 0.00215(8)
CrZ 0.00414(10) 0.00464(10) 0.00480(8) 0.00033(7) -0.00014(6) 0.00215(8)
B 0.0054(5) 0.0056(6) 0.0080(6) 0.0008(5) 0.0004(2) 0.0028(3)
```

```
Si 0.00451(13) 0.00431(12) 0.00567(12) -0.00035(9) -0.00024(10) 0.00208(9)
O1 0.0048(5) 0.0048(5) 0.0080(8) 0.000 0.000 0.0024(2)
O2 0.0044(3) 0.0041(4) 0.0074(5) 0.0013(3) 0.00066(17) 0.0021(2)
O3 0.0096(5) 0.0089(4) 0.0062(4) 0.00064(18) 0.0013(4) 0.0048(2)
O4 0.0068(3) 0.0150(5) 0.0083(4) -0.0004(4) -0.0002(2) 0.0075(3)
O5 0.0138(5) 0.0060(3) 0.0081(4) 0.00035(19) 0.0007(4) 0.0069(3)
O6 0.0075(3) 0.0060(3) 0.0046(3) -0.0005(2) -0.0001(2) 0.0030(3)
O7 0.0067(3) 0.0059(3) 0.0084(3) -0.0015(3) -0.0016(3) 0.0011(3)
O8 0.0051(3) 0.0085(3) 0.0132(3) 0.0035(3) 0.0007(3) 0.0034(3)

_geom_special_details
;
 All esds (except the esd in the dihedral angle between two l.s. planes)
 are estimated using the full covariance matrix.  The cell esds are taken
 into account individually in the estimation of esds in distances, angles
 and torsion angles; correlations between esds in cell parameters are only
 used when they are defined by crystal symmetry.  An approximate (isotropic)
 treatment of cell esds is used for estimating esds involving l.s. planes.
;

loop_
 _geom_bond_atom_site_label_1
 _geom_bond_atom_site_label_2
 _geom_bond_distance
 _geom_bond_site_symmetry_2
 _geom_bond_publ_flag
NaX O2 2.5707(15) . ?
NaX O2 2.5708(15) 3 ?
NaX O2 2.5708(15) 2 ?
NaX O5 2.7338(12) 3 ?
NaX O5 2.7338(12) . ?
NaX O5 2.7339(12) 2 ?
NaX O4 2.8243(13) 3 ?
NaX O4 2.8244(13) . ?
NaX O4 2.8244(13) 2 ?
NaX Si 3.4688(8) 2 ?
NaX Si 3.4688(8) 5 ?
NaX Si 3.4688(8) 4 ?
CrY O1 1.9530(9) . ?
CrY O6 1.9798(8) 6 ?
CrY O6 1.9798(8) . ?
CrY O2 2.0168(7) . ?
CrY O2 2.0168(7) 3 ?
CrY O3 2.0744(11) . ?
CrY CrY 2.9746(4) 2 ?
CrY CrY 2.9747(4) 3 ?
CrY MgZ 3.0455(3) 6 ?
CrY MgZ 3.0455(3) . ?
MgZ O8 1.9660(8) 8 ?
MgZ O8 1.9714(8) . ?
MgZ O7 1.9824(8) 8 ?
MgZ O6 2.0073(8) . ?
MgZ O7 2.0079(8) 15 ?
MgZ O3 2.0463(6) . ?
MgZ MgZ 3.0086(2) 15_554 ?
```

```
MgZ CrZ 3.0086(2) 15_554 ?
MgZ MgZ 3.0086(2) 8 ?
MgZ CrZ 3.0086(2) 8 ?
MgZ Si 3.2543(4) 8 ?
B O8 1.3624(11) . ?
B O8 1.3624(11) 5 ?
B O2 1.398(2) . ?
Si O7 1.5997(7) . ?
Si O6 1.6156(8) 1_554 ?
Si O4 1.6277(5) . ?
Si O5 1.6427(5) . ?
Si MgZ 3.2542(4) 15_554 ?
Si MgZ 3.2652(3) 8_554 ?
O1 CrY 1.9529(9) 2 ?
O1 CrY 1.9530(9) 3 ?
O2 CrY 2.0168(7) 2 ?
O3 CrZ 2.0463(6) 6 ?
O3 MgZ 2.0463(6) 6 ?
O3 H3 0.98(2) . ?
O4 Si 1.6276(5) 5 ?
O5 Si 1.6428(5) 6 ?
O6 Si 1.6156(8) 1_556 ?
O7 CrZ 1.9824(8) 15_554 ?
O7 MgZ 1.9824(8) 15_554 ?
O7 MgZ 2.0080(8) 8_554 ?
O7 CrZ 2.0080(8) 8_554 ?
O8 CrZ 1.9661(8) 15_554 ?
O8 MgZ 1.9661(8) 15_554 ?

loop_
 _geom_angle_atom_site_label_1
 _geom_angle_atom_site_label_2
 _geom_angle_atom_site_label_3
 _geom_angle
 _geom_angle_site_symmetry_1
 _geom_angle_site_symmetry_3
 _geom_angle_publ_flag
O2 NaX O2 68.87(5) . 3 ?
O2 NaX O2 68.87(5) . 2 ?
O2 NaX O2 68.87(5) 3 2 ?
O2 NaX O5 152.42(6) . 3 ?
O2 NaX O5 88.63(3) 3 3 ?
O2 NaX O5 88.63(3) 2 3 ?
O2 NaX O5 88.63(3) . . ?
O2 NaX O5 88.63(3) 3 . ?
O2 NaX O5 152.42(6) 2 . ?
O5 NaX O5 107.20(4) 3 . ?
O2 NaX O5 88.63(3) . 2 ?
O2 NaX O5 152.42(6) 3 2 ?
O2 NaX O5 88.63(3) 2 2 ?
O5 NaX O5 107.20(4) 3 2 ?
O5 NaX O5 107.20(4) . 2 ?
O2 NaX O4 127.28(3) . 3 ?
O2 NaX O4 73.17(3) 3 3 ?
O2 NaX O4 127.28(3) 2 3 ?
```

```
O5 NaX O4 54.938(14) 3 3 ?
O5 NaX O4 54.937(14) . 3 ?
O5 NaX O4 134.40(6) 2 3 ?
O2 NaX O4 73.17(3) . . ?
O2 NaX O4 127.28(3) 3 . ?
O2 NaX O4 127.28(3) 2 . ?
O5 NaX O4 134.40(6) 3 . ?
O5 NaX O4 54.937(14) . . ?
O5 NaX O4 54.937(14) 2 . ?
O4 NaX O4 104.66(4) 3 . ?
O2 NaX O4 127.28(3) . 2 ?
O2 NaX O4 127.28(3) 3 2 ?
O2 NaX O4 73.17(3) 2 2 ?
O5 NaX O4 54.937(14) 3 2 ?
O5 NaX O4 134.40(6) . 2 ?
O5 NaX O4 54.936(14) 2 2 ?
O4 NaX O4 104.66(4) 3 2 ?
O4 NaX O4 104.66(4) . 2 ?
O2 NaX Si 111.154(12) . 2 ?
O2 NaX Si 149.63(3) 3 2 ?
O2 NaX Si 82.65(2) 2 2 ?
O5 NaX Si 80.11(2) 3 2 ?
O5 NaX Si 121.60(4) . 2 ?
O5 NaX Si 27.602(11) 2 2 ?
O4 NaX Si 120.05(5) 3 2 ?
O4 NaX Si 78.36(2) . 2 ?
O4 NaX Si 27.625(11) 2 2 ?
O2 NaX Si 82.65(2) . 5 ?
O2 NaX Si 149.63(3) 3 5 ?
O2 NaX Si 111.153(12) 2 5 ?
O5 NaX Si 121.60(4) 3 5 ?
O5 NaX Si 80.11(2) . 5 ?
O5 NaX Si 27.602(11) 2 5 ?
O4 NaX Si 120.05(5) 3 5 ?
O4 NaX Si 27.626(11) . 5 ?
O4 NaX Si 78.36(2) 2 5 ?
Si NaX Si 51.213(14) 2 5 ?
O2 NaX Si 149.63(3) . 4 ?
O2 NaX Si 111.152(12) 3 4 ?
O2 NaX Si 82.65(2) 2 4 ?
O5 NaX Si 27.598(11) 3 4 ?
O5 NaX Si 121.60(4) . 4 ?
O5 NaX Si 80.11(2) 2 4 ?
O4 NaX Si 78.36(2) 3 4 ?
O4 NaX Si 120.05(5) . 4 ?
O4 NaX Si 27.629(11) 2 4 ?
Si NaX Si 52.698(15) 2 4 ?
Si NaX Si 98.70(3) 5 4 ?
O1 CrY O6 99.58(4) . 6 ?
O1 CrY O6 99.59(4) . . ?
O6 CrY O6 88.97(4) 6 . ?
O1 CrY O2 82.75(4) . . ?
O6 CrY O2 177.32(4) 6 . ?
O6 CrY O2 89.36(4) . . ?
O1 CrY O2 82.75(4) . 3 ?
```

```
O6 CrY O2 89.36(4) 6 3 ?
O6 CrY O2 177.32(4) . 3 ?
O2 CrY O2 92.24(6) . 3 ?
O1 CrY O3 179.02(6) . . ?
O6 CrY O3 79.73(3) 6 . ?
O6 CrY O3 79.73(3) . . ?
O2 CrY O3 97.92(3) . . ?
O2 CrY O3 97.92(3) 3 . ?
O1 CrY CrY 40.40(3) . 2 ?
O6 CrY CrY 139.75(2) 6 2 ?
O6 CrY CrY 93.58(2) . 2 ?
O2 CrY CrY 42.48(2) . 2 ?
O2 CrY CrY 89.04(3) 3 2 ?
O3 CrY CrY 140.22(2) . 2 ?
O1 CrY CrY 40.40(3) . 3 ?
O6 CrY CrY 93.58(2) 6 3 ?
O6 CrY CrY 139.75(2) . 3 ?
O2 CrY CrY 89.04(3) . 3 ?
O2 CrY CrY 42.48(2) 3 3 ?
O3 CrY CrY 140.22(2) . 3 ?
CrY CrY CrY 60.0 2 3 ?
O1 CrY MgZ 137.56(2) . 6 ?
O6 CrY MgZ 40.53(2) 6 6 ?
O6 CrY MgZ 94.32(2) . 6 ?
O2 CrY MgZ 137.60(2) . 6 ?
O2 CrY MgZ 83.05(3) 3 6 ?
O3 CrY MgZ 41.991(15) . 6 ?
CrY CrY MgZ 172.097(5) 2 6 ?
CrY CrY MgZ 113.227(5) 3 6 ?
O1 CrY MgZ 137.56(2) . . ?
O6 CrY MgZ 94.32(2) 6 . ?
O6 CrY MgZ 40.53(2) . . ?
O2 CrY MgZ 83.05(3) . . ?
O2 CrY MgZ 137.59(2) 3 . ?
O3 CrY MgZ 41.992(15) . . ?
CrY CrY MgZ 113.230(5) 2 . ?
CrY CrY MgZ 172.099(5) 3 . ?
MgZ CrY MgZ 73.182(9) 6 . ?
O1 CrY NaX 88.92(5) . . ?
O6 CrY NaX 134.17(2) 6 . ?
O6 CrY NaX 134.17(2) . . ?
O2 CrY NaX 46.86(3) . . ?
O2 CrY NaX 46.86(3) 3 . ?
O3 CrY NaX 92.06(4) . . ?
CrY CrY NaX 64.752(10) 2 . ?
CrY CrY NaX 64.752(10) 3 . ?
MgZ CrY NaX 109.281(12) 6 . ?
MgZ CrY NaX 109.281(12) . . ?
O8 MgZ O8 172.72(3) 8 . ?
O8 MgZ O7 95.09(3) 8 8 ?
O8 MgZ O7 79.28(3) . 8 ?
O8 MgZ O6 94.90(3) 8 . ?
O8 MgZ O6 90.94(3) . . ?
O7 MgZ O6 169.76(3) 8 . ?
O8 MgZ O7 78.78(3) 8 15 ?
```

```
O8 MgZ O7 96.56(3) . 15 ?
O7 MgZ O7 90.771(12) 8 15 ?
O6 MgZ O7 93.35(3) . 15 ?
O8 MgZ O3 98.08(4) 8 . ?
O8 MgZ O3 87.23(4) . . ?
O7 MgZ O3 96.60(4) 8 . ?
O6 MgZ O3 79.77(4) . . ?
O7 MgZ O3 172.24(4) 15 . ?
O8 MgZ MgZ 133.14(3) 8 15_554 ?
O8 MgZ MgZ 40.11(2) . 15_554 ?
O7 MgZ MgZ 41.38(2) 8 15_554 ?
O6 MgZ MgZ 129.78(2) . 15_554 ?
O7 MgZ MgZ 84.51(2) 15 15_554 ?
O3 MgZ MgZ 102.64(3) . 15_554 ?
O8 MgZ CrZ 133.14(3) 8 15_554 ?
O8 MgZ CrZ 40.11(2) . 15_554 ?
O7 MgZ CrZ 41.38(2) 8 15_554 ?
O6 MgZ CrZ 129.78(2) . 15_554 ?
O7 MgZ CrZ 84.51(2) 15 15_554 ?
O3 MgZ CrZ 102.64(3) . 15_554 ?
MgZ MgZ CrZ 0.000(12) 15_554 15_554 ?
O8 MgZ MgZ 40.24(2) 8 8 ?
O8 MgZ MgZ 136.45(3) . 8 ?
O7 MgZ MgZ 104.04(2) 8 8 ?
O6 MgZ MgZ 85.10(2) . 8 ?
O7 MgZ MgZ 40.75(2) 15 8 ?
O3 MgZ MgZ 134.04(3) . 8 ?
MgZ MgZ MgZ 120.012(9) 15_554 8 ?
CrZ MgZ MgZ 120.012(9) 15_554 8 ?
O8 MgZ CrZ 40.24(2) 8 8 ?
O8 MgZ CrZ 136.45(3) . 8 ?
O7 MgZ CrZ 104.04(2) 8 8 ?
O6 MgZ CrZ 85.10(2) . 8 ?
O7 MgZ CrZ 40.75(2) 15 8 ?
O3 MgZ CrZ 134.04(3) . 8 ?
MgZ MgZ CrZ 120.012(9) 15_554 8 ?
CrZ MgZ CrZ 120.012(9) 15_554 8 ?
MgZ MgZ CrZ 0.0 8 8 ?
O8 MgZ CrY 110.05(2) 8 . ?
O8 MgZ CrY 77.23(2) . . ?
O7 MgZ CrY 133.21(3) 8 . ?
O6 MgZ CrY 39.86(2) . . ?
O7 MgZ CrY 131.58(2) 15 . ?
O3 MgZ CrY 42.70(3) . . ?
MgZ MgZ CrY 113.723(10) 15_554 . ?
CrZ MgZ CrY 113.723(10) 15_554 . ?
MgZ MgZ CrY 120.818(9) 8 . ?
CrZ MgZ CrY 120.818(9) 8 . ?
O8 MgZ Si 77.66(3) 8 8 ?
O8 MgZ Si 97.87(2) . 8 ?
O7 MgZ Si 22.03(2) 8 8 ?
O6 MgZ Si 162.73(2) . 8 ?
O7 MgZ Si 100.32(2) 15 8 ?
O3 MgZ Si 85.82(3) . 8 ?
MgZ MgZ Si 62.701(7) 15_554 8 ?
```

```
CrZ MgZ Si 62.701(7) 15_554 8 ?
MgZ MgZ Si 98.375(10) 8 8 ?
CrZ MgZ Si 98.375(10) 8 8 ?
CrY MgZ Si 128.068(9) . 8 ?
O8 B O8 119.64(14) . 5 ?
O8 B O2 120.18(7) . . ?
O8 B O2 120.18(7) 5 . ?
O7 Si O6 110.86(4) . 1_554 ?
O7 Si O4 110.44(5) . . ?
O6 Si O4 111.31(5) 1_554 . ?
O7 Si O5 110.78(5) . . ?
O6 Si O5 109.91(4) 1_554 . ?
O4 Si O5 103.31(6) . . ?
O7 Si MgZ 27.69(3) . 15_554 ?
O6 Si MgZ 131.32(3) 1_554 15_554 ?
O4 Si MgZ 84.08(4) . 15_554 ?
O5 Si MgZ 110.65(4) . 15_554 ?
O7 Si MgZ 28.41(3) . 8_554 ?
O6 Si MgZ 83.35(3) 1_554 8_554 ?
O4 Si MgZ 130.08(4) . 8_554 ?
O5 Si MgZ 116.29(4) . 8_554 ?
MgZ Si MgZ 54.963(5) 15_554 8_554 ?
O7 Si NaX 131.73(4) . . ?
O6 Si NaX 117.36(3) 1_554 . ?
O4 Si NaX 53.58(4) . . ?
O5 Si NaX 50.45(4) . . ?
MgZ Si NaX 108.92(2) 15_554 . ?
MgZ Si NaX 157.41(2) 8_554 . ?
CrY O1 CrY 99.21(6) 2 . ?
CrY O1 CrY 99.21(6) 2 3 ?
CrY O1 CrY 99.21(6) . 3 ?
B O2 CrY 120.16(5) . 2 ?
B O2 CrY 120.16(5) . . ?
CrY O2 CrY 95.03(5) 2 . ?
B O2 NaX 119.70(9) . . ?
CrY O2 NaX 98.22(4) 2 . ?
CrY O2 NaX 98.22(4) . . ?
CrZ O3 MgZ 0.000(6) 6 6 ?
CrZ O3 MgZ 125.04(6) 6 . ?
MgZ O3 MgZ 125.04(6) 6 . ?
CrZ O3 CrY 95.30(4) 6 . ?
MgZ O3 CrY 95.30(4) 6 . ?
MgZ O3 CrY 95.30(4) . . ?
CrZ O3 H3 112.1(3) 6 . ?
MgZ O3 H3 112.1(3) 6 . ?
MgZ O3 H3 112.1(3) . . ?
CrY O3 H3 113.9(12) . . ?
Si O4 Si 142.12(8) 5 . ?
Si O4 NaX 98.80(4) 5 . ?
Si O4 NaX 98.80(4) . . ?
Si O5 Si 131.73(7) . 6 ?
Si O5 NaX 101.95(4) . . ?
Si O5 NaX 101.95(4) 6 . ?
Si O6 CrY 124.94(4) 1_556 . ?
Si O6 MgZ 128.78(5) 1_556 . ?
```

```
CrY O6 MgZ 99.61(4) . . ?
Si O7 CrZ 130.28(5) . 15_554 ?
Si O7 MgZ 130.28(5) . 15_554 ?
CrZ O7 MgZ 0.000(12) 15_554 15_554 ?
Si O7 MgZ 129.31(5) . 8_554 ?
CrZ O7 MgZ 97.86(3) 15_554 8_554 ?
MgZ O7 MgZ 97.86(3) 15_554 8_554 ?
Si O7 CrZ 129.31(5) . 8_554 ?
CrZ O7 CrZ 97.86(3) 15_554 8_554 ?
MgZ O7 CrZ 97.86(3) 15_554 8_554 ?
MgZ O7 CrZ 0.00(3) 8_554 8_554 ?
B O8 CrZ 134.18(8) . 15_554 ?
B O8 MgZ 134.18(8) . 15_554 ?
CrZ O8 MgZ 0.00(2) 15_554 15_554 ?
B O8 MgZ 125.61(8) . . ?
CrZ O8 MgZ 99.65(3) 15_554 . ?
MgZ O8 MgZ 99.65(3) 15_554 . ?

_diffrn_measured_fraction_theta_max     0.958
_diffrn_reflns_theta_full               37.05
_diffrn_measured_fraction_theta_full    0.958
_refine_diff_density_max      0.353
_refine_diff_density_min     -0.363
_refine_diff_density_rms      0.064
```